Journal Homepage: -www.journalijar.com

INTERNATIONAL JOURNAL OF ADVANCED RESEARCH (IJAR)

Article DOI : 10.21474/IJAR01/22862
DOI URL : http://dx.doi.org/10.21474/IJAR01/22862

ISSN (O): 2320-5407
ISSN (P): 3107-4928

RESEARCH ARTICLE

MODELING THE IMPACT OF PIER TYPE ON THE RELATIVE POWER-REDUCTION FACTOR OF A PV GENERATOR

Maibigue Nanglet[1], Arafat Ousman Bechir[2] and Mahamat Hassan Bechir[2]

1. Faculty of Exact and Applied Sciences of Farcha -University of Ndjamena, Chad.
2. National Institute of Higher Sciences and Technologies of Abeche, Chad.

Manuscript Info

Manuscript History
Received: 16 December 2025
Final Accepted: 18 January 2026
Published: February 2026

Key words:-
Modeling – Power Loss – Pier convection – PV Generator.

Abstract

This paper models and simulates the impact of various trellis materials (reinforced concrete, iron, steel, aluminum, sand, earth, gravel, water, seckho, baked brick, air, and straw) on the power output of a photovoltaic generator (PVG). The aim of this work is to quantify power losses caused by Back Surface Field (BSF) heating induced by each support type. Simulations were conducted over 5, 10, 15, 20, and 25 years across multiple installation sites. Results show that, after 5 years, trellis materials reduce PV power by 21.42% to 27.60%, depending on the pier type. Average long term losses reached 20.90% (5 years), 20.01% (10 years), 23.01% (15 years), 22.25% (20 years), and 21.53% (25 years), with air suspended and water based installations performing best.

Introduction: -

Experiments have shown that after prolonged exposure to natural climatic conditions, thermal stresses and a deterioration in the electrical performance of photovoltaic modules are observed [[1]- [4]]. Therefore, a thorough analysis of the causes of the reduction in maximum power and the aging of PV systems is necessary. Such an analysis inevitably involves studying the degradation of the I-V curve due to the effects of the mounting structure or site-specific factors (surface: concrete, sheet metal, metal, wood, planks, seckho, sand, water, vegetation, etc.) on PV modules installed in a harsh environment.Let us recall that the metallic contacts on the emitter and the substrate serve to collect the photogenerated carrier current; the contacts must be ohmic [[5]- [17]]. The rear surface (full metallization) of the solar cell is characterized by a very high surface recombination velocity. The back surface electric field (Back Surface Field, BSF) involves creating a potential barrier (for example, a p+-p or n+-n junction) on the rear side to ensure passivation.The potential barrier induced by the difference in doping levels between the base and the BSF tends to confine minority carriers within the base. As a result, they are kept away from the rear surface. Therefore, the absence of an electric field at the rear surface near the ohmic contact causes the minority carriers to be drawn into the space charge region, leading to poor collection. This results in a deterioration of photocurrent, open-circuit voltage, and photovoltaic conversion efficiency [[13], [15], [18], [19]]. The objective of this study is to analyze the modeled power evolution of a photovoltaic system installed on different trestle structures. To achieve this, the work is organized into three main sections. First presents and explains the physical influence of trestles on solar cell behavior. Second details the mathematical formulations and material parameters used in the

Corresponding Author: -Maibigue Nanglet
Address: -Faculty of Exact and Applied Sciences of Farcha -University of Ndjamena, Chad.

modeling process. And third provides the simulation results followed by a comprehensive discussion of the findings [[20]– [23]].

Degradation of the PV module: -

Published data on photovoltaic (PV) degradation rates have been compiled and re-evaluated, revealing a sharp rise in research interest in recent years. Nearly 200 studies conducted across 40 countries now report more than 11,000 individual degradation rates. This extensive body of work, documented by Dirk Jordan et al., provides one of the most comprehensive global assessments of PV performance decline to date [[2], [11], [16]].

Factors of cell degradation: -

The degradation mechanisms in photovoltaic modules operating in harsh environments, linking declines in short-circuit current, open-circuit voltage and fill factor to changes in intrinsic cell properties (reverse saturation current, ideality factor) and parasitic resistances. High temperature and humidity accelerate chemical and optical damage—especially EVA encapsulant discoloration—that reduces photon transmission and lowers short-circuit current and output power, while environmental stressors increase dust accumulation whose effect depends on particle characteristics and local climate. Recent reports, including studies from Iraq, document soiling-related energy losses up to 70%, highlighting severe site-dependent performance impacts. Despite evidence of climate- and racking-dependent degradation rates, manufacturers have been reluctant to adopt racking-based warranties, underlining the need for comprehensive global assessments to quantify degradation differences and support warranty frameworks [[16], [18]- [19], [30]].

Mathematical formalism for evaluating PV degradation: -

Photovoltaic Generator (PVG): -

This work examines the specific site factor (τ_{fss}), which quantifies structural-induced losses in photovoltaic generators by modifying photocurrent and influencing carrier transport parameters. Surface losses are modeled through recombination rates that reflect the quality of the cell interfaces. The solar cell base is represented as two regions, including a heavily doped rear zone that introduces a minor energy barrier. This configuration enhances minority-carrier confinement and enables recovery of carriers typically lost in simpler cells. Rear-surface losses are finally expressed through the recombination current at the ohmic contact, as defined by equations [[2], [15], [31]]:

$$I = [I_{Phref} - K_i.(T - T_{ref})].\frac{\varepsilon_{fss}.G}{G_{Ref}} - I_0.\left[\exp\left(\frac{(V+R_S.I)}{m.V_t}\right) - 1\right] - \frac{(V+R_S.I)}{R_P}.\left[1 + a\left(1 - \frac{(V+R_S.I)^{-n}}{V_b}\right)\right] \quad (1)$$

$$T = \left[\frac{NOCT - 20}{0.8}\right].G + T_{amb} \quad (2)$$

T: is the temperature under normal NOCT conditions, T_{amb} (patterns T)

This equation describes the current flowing through the solar cell by applying Kirchhoff's law.

$$G = 1000\frac{W}{m^2}, T = 25°C, AM = 1.5, I_m \approx 0.8.I_{CC} \text{ et } V_m \approx 0.8V_{CO} \quad (3)$$

The temporary degradation rate (τ_{fss})due to the specific site factor (x) is given by:

$$\tau_{fss}(\%) = \left(1 - \frac{X_{mes}}{X_m}\right).100 \text{ et } \tau_d = \left(\frac{\tau_{fss}(\%)}{t_{expo}}\right) \quad (4)$$

GPV Power Losses: -

In this section, we present the modeling approach used in the study. The analysis incorporates installation duration, PV technology, electrical characteristics, site-specific conditions, and the cell's orientation angle. We varied the site factor by testing different support materials (reinforced concrete, sheet metal, tile, backsheet, earth, sand, water, straw, aluminum, soil, diatomaceous earth, natron, clay, plastic, glass, and vacuum) while keeping the PV system unchanged.

Materials and Methods: -

Module & Simulation Parameters: -

Module power [W]: P_{STC} = 300 Wc;

This paper develops a long-term performance model for photovoltaic (PV) systems that integrates irradiance, temperature, and material-dependent thermal behavior. Each pier type—concrete, metal, sand, earth, water, and air—is defined by its thermal conductivity and heat-retention properties, which govern Back Surface Field (BSF) temperature and consequently influence PV output. The model couples standard PV electrical equations with site-specific thermal simulations to isolate the thermal impact of support structures. Power degradation is evaluated over 5-, 10-, 15-, 20-, and 25-year intervals under Sahelian environmental conditions (Chad). Identical PV

technology and geometry are assumed to ensure that performance differences arise solely from pier-material effects [[6]- [12]].

Irradiance per day (G):

-$G_{max} = \sin(h_{pro}) + T_{var}$, with: $G_{maw} = \frac{1000}{W/m^2}peak$ (5)

-Daily factor (d_{fac}):

$d_{fac} = 1 + 0.2 * \sin(2\pi * t_{year})$; (6)

-Seasonal patterns (T_{var}):

$T_{var}(\pm\frac{h_d}{20}) = mod(t, 24)$; (7)

$G = G_{max} . \max[0, \sin\left(\frac{\pi * h}{12}\right)] * d_{fac}$ (8)

-External temperature (T_{amb}):

$T_{amb} = T_{amb,mean} + T_{amb,se} * \sin(2\pi * t_{year} - 0.5) + T_{amb,d} * \sin(\frac{2\pi * h}{24})$ (9)

Note 1:t_{year} (step time), h_d(day hour), $T_{amb,se}$(seasonal (T_{amb}), d(day), h_{pro} (hour profile).

Table 1. Table of substrates (assumptions)

This table summarizes the assumed thermal and physical properties of the different substrate materials used in the PV system analysis [8].

Name	ΔTeff(°C at 1000W/m^2)	Soiling rate (1/year)	Max.soiling (fraction)	Corrosion-rate(annual fraction
Standard polymer backsheet (Tedlar-PET-Tedlar)	+1.500	0.600	0.180	0.012
Glass-glass module	−0.800	0.400	0.120	0.002
Glass + polymer backsheet (tempered front)	+0.300	0.500	0.150	0.008
Metal-backed (aluminum) substrate	−1.200	0.700	0.200	0.020
Galvanized steel-backed substrate	−0.500	0.800	0.220	0.030
Flexible thin-film polymer (flexible module)	+2.000	0.900	0.250	0.015
Anti-soiling / hydrophobic coated glass	−0.100	0.150	0.050	0.003
Textured / high-emissivity glass	−0.300	0.450	0.100	0.005
Polymer backsheet with ventilated gap	+1.800	0.550	0.160	0.010
BIPV integrated membrane (roof-integrated)	+2.500	0.350	0.140	0.025

-Instantaneous power calculations for each substrate, considering the influence of soiling(s_o):

$$\begin{cases} fork = 1:n, \quad n \epsilon N \\ s_o = s_o(k) \end{cases} \quad (10)$$

$T_{cell} = T_{amb} + \frac{(NOCT-20)}{800} * G + s_{o\,eff}\frac{G}{1000}$ (11)

-Cumulative soiling over time:

$s_{o\,frac}(t) = max(s_o(1 - e^{(-s_o * t_{year})}))\ and s_{o\,frac,t} = s_o max(s_o(1 - e^{(-s_o * t_{year})}))$ (12)

$tot_{rate} = intsec_{rate} + s_o * Cor_{rate}$ with $d_{fac} = e^{(-tot_{rate} * t_{year})}$(14)

-Annual multiplicative degradation, combining intrinsic aging and corrosion effects applied progressively over time:

$d_{fac} = e^{(t_{year} * ln(1 - tot_{rate}))}$, $tot_{rate} = intsec_{rate} + s_o * Cor_{rat}$ (13)

- Instantaneous power (P_{ins}):

$P = P_{STC} * (\frac{G}{1000}) * (1 + t_{coef} .* (T_{cell} - 25)) * (1 - s_{o\,frac}(t)) * d_{fac}$(14)

$P_{ins} = P_{STC} .* \left(\frac{G}{1000}\right)\left(1 + t_{coef} .* (T_{cell} - 25)\right) .* \left(1 - s_{o\,frac,t}(t)\right) .* d_{fac}$ (15)

Note 2: d_{fac} (degree factor), s_o(soiling), tot_{rate}(total rate), int_{srat}(intrinsic degre rate), Cor_{rat}(corrosion rate), eff(efficient), T_{cell}(cell temperature), $s_{o_{eff}}$(soiling delta$T_{efficient}$), $s_{o_{frac,t}}$(soiling fractor max).

Equipment: -

This paragraph examines the various platforms used for installing photovoltaic systems. The encapsulation of thin-film PV modules is essential for ensuring long-term reliability and durability.

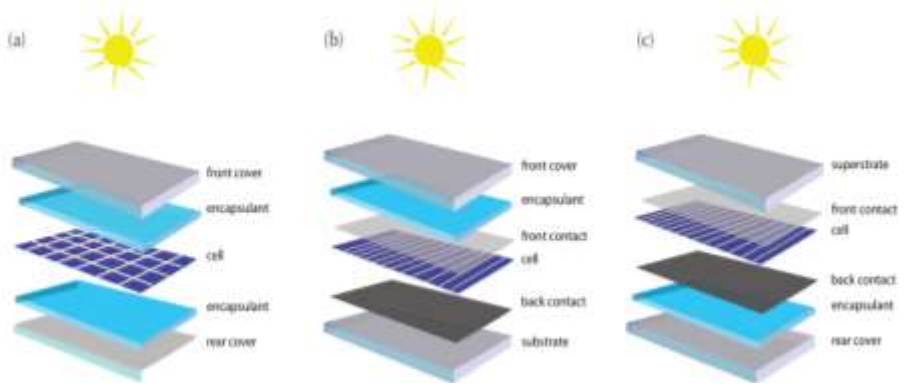

Figure1.(a) General set-up Ac-Si PV module; (b) substrate-type thin-film PV module; (c) superstrate-type thin-film PV module [[3], [10]].

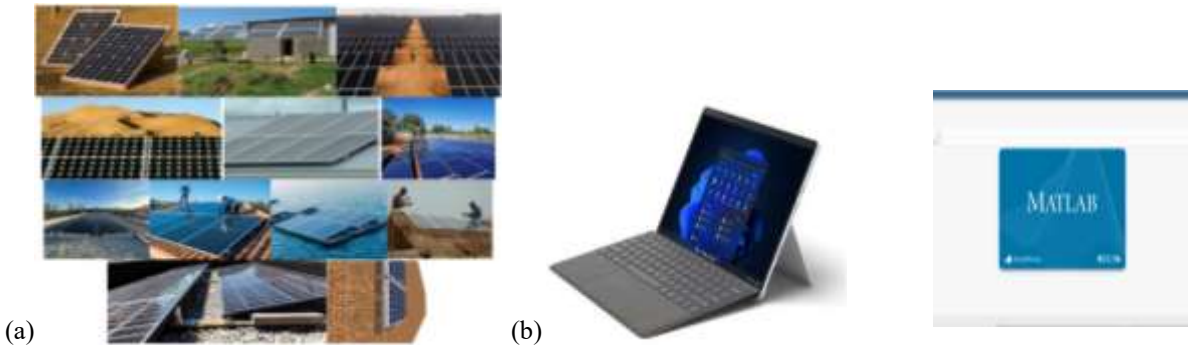

Figure 2. (a) Different types of photovoltaic installation racks (priers) (b)Tools work space Computer: Surface Go I5 10th Generation N2B2UOM

Results and Discussion: -

This section presents the results of our simulation

Simulation of the relative power of the GPV according to different piers: -

The figure below shows that the power is affected by the site characteristics on which a PV system is installed and by its lifespan. The delamination near racks reduces heat conduction to the backsheet, increasing cell back sheet field temperature difference.

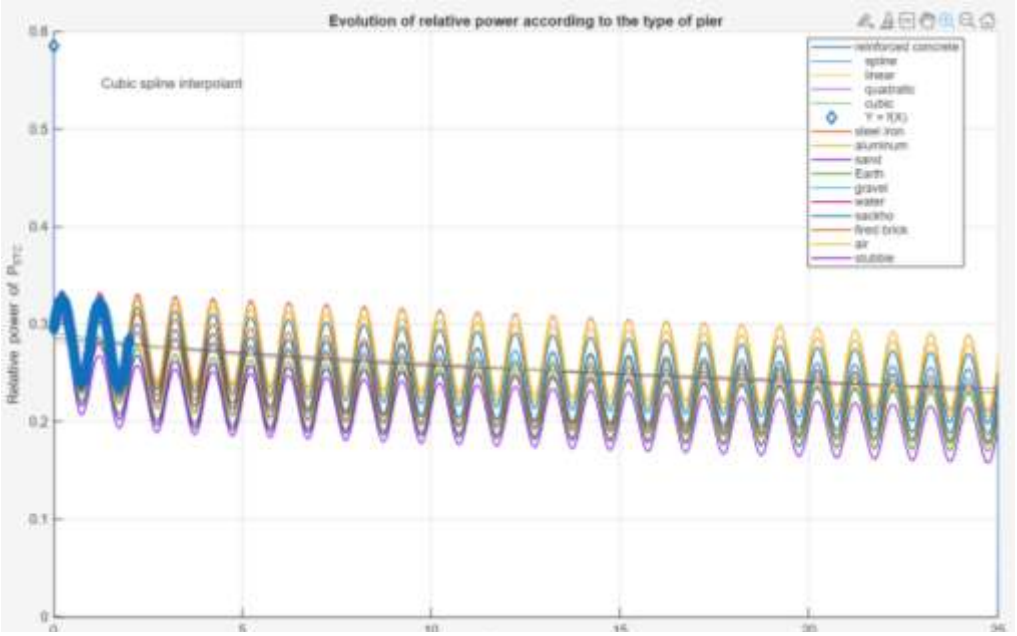

Figure 4. Evolution of relative power according to the type of piers

Figure 4 illustrates the impact of various pier materials on the relative power P_{STC} of a photovoltaic system. Iron, aluminum, and gravel supports exhibit the highest power losses, accelerating PV module degradation and contributing to the failure of associated static converters. These results highlight the importance of carefully selecting installation sites, whereas in sub-Saharan Africa—particularly in Chad—panels are often placed directly on the ground or on metal roofs. The figure also shows that voltage drops caused by pier effects intensify over time. Elevated temperature differences ΔT between the cell and backsheet, especially near rack attachment points, further amplify these losses. Thermographic or contact-sensor measurements confirm these localized thermal stresses, underscoring their role in long-term performance decline.

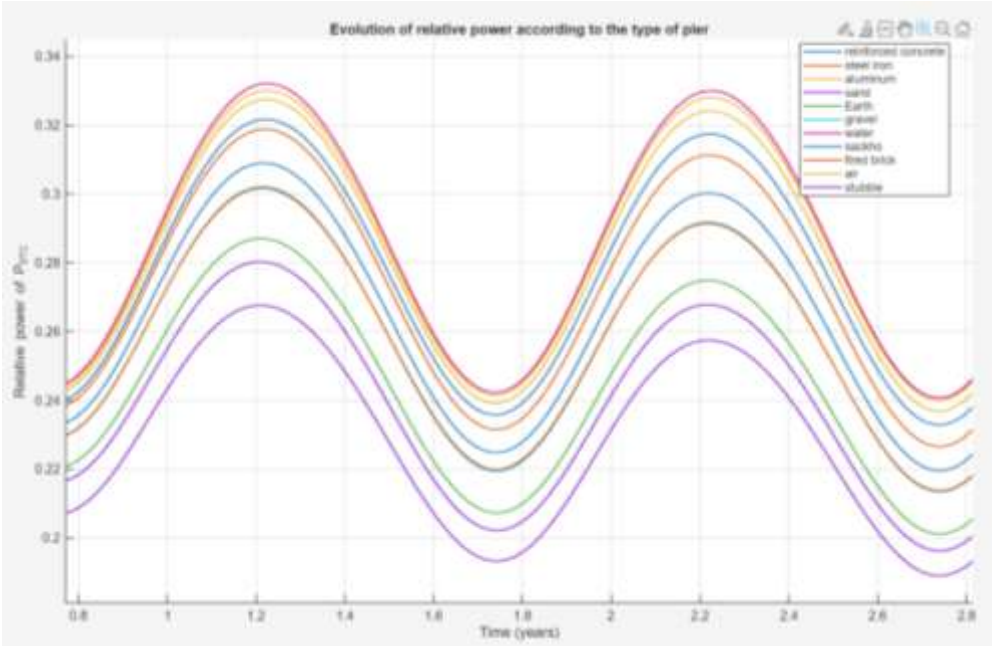

Figure 5. Zoom on the influence of different jetties

In this Figure 5, we observe that the PV system loses more of its performance when installed on sand, straw, and soil. This can be explained by the fact that the Sahelian climate, coupled with the thermoelectric properties of these sites (sand, straw, and soil), affects the performance of the PV system.Fouling and contact occlusions increase thermal time constant of substrate zones near racks.

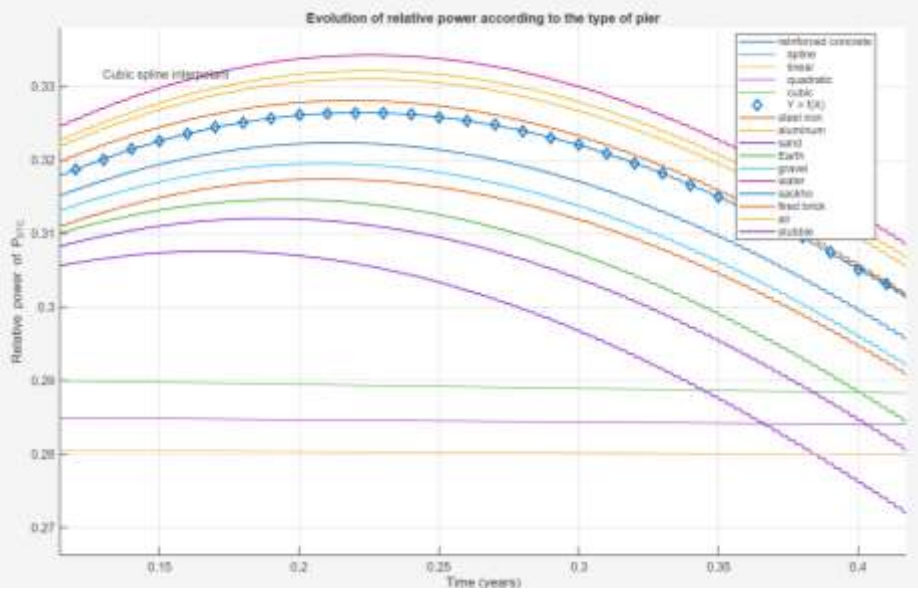

Figure 6. Permissible range of pier installation areas

Figure 6 shows the range of acceptable piers for the installation of a photovoltaic generator without significant relative reduction power factor. To outline these areas, we drew a line using the geometric regression law y = f(x) based on the simulated data.

Thus, this curve serves as a boundary: above it, conditions are considered favorable for optimal efficiency. Conversely, sites located below the line y = f(x) show insufficient performance and are not recommended. The position of a point relative to the line takes into account factors such as the angle of incidence, reflection, and environmental absorption. We have identified several materials and surfaces (piers) that enhance capture and minimize losses.Reinforced concrete, for example, provides a stable and reflective surface that limits the effects of local shading. Aluminum offers good reflectivity and durability, supporting consistent performance. Fired brick combines thermal inertia with a texture suitable for long-lasting installation. Water, when present in a calm and reflective form, can increase the received irradiation through reflection. Air, understood here as open areas without obstacles, reduces losses related to shading and diffusion. Consequently, we recommend installing PV generators on these supports or in these environments when conditions allow. For sites below y = f(x), corrective measures (elevation, change of orientation, or surface treatment) are necessary before installation.

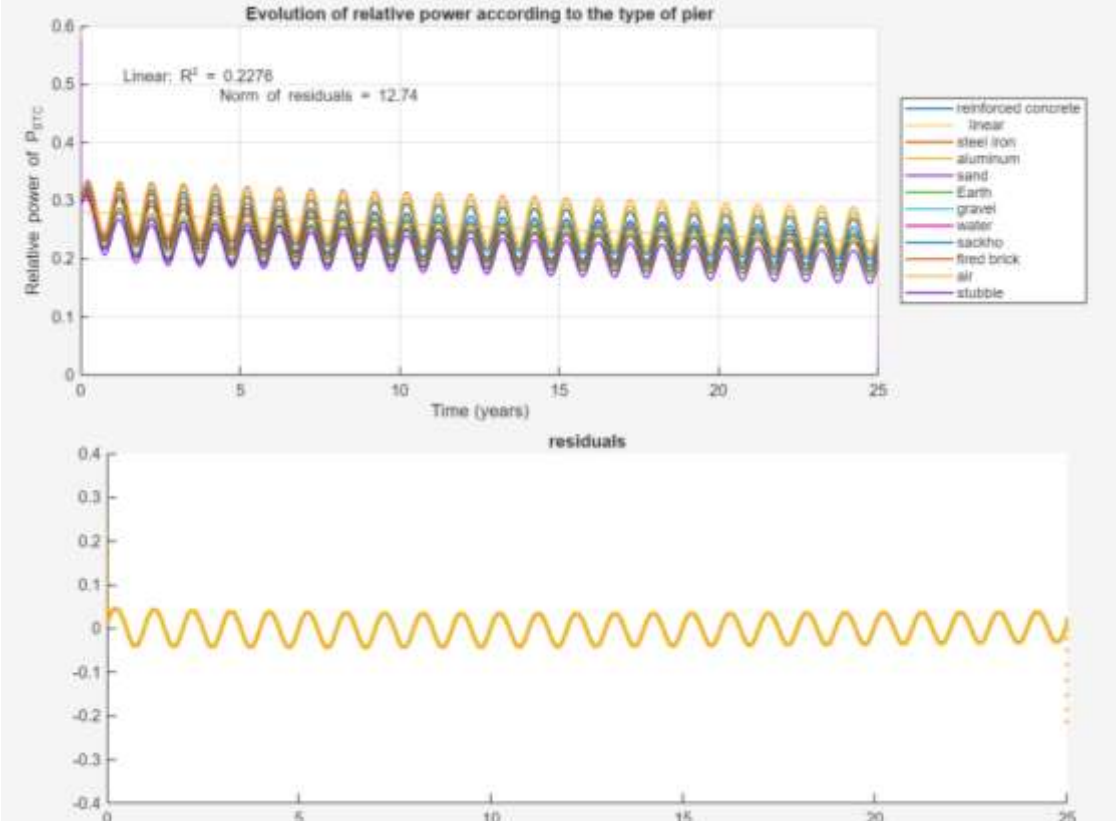

Figure 7. Range of the favorable zone over 25 years

The figure 7 evaluates the long-term performance of photovoltaic (PV) installations mounted on various structural supports. Over a 25-year period, reinforced concrete, aluminum, air, and water-based sites consistently remained the most favorable for PV operation. The analysis shows that moisture retention and fouling at rack interfaces accelerate corrosion and delamination, increasing thermal coupling to the cells and generating temperature shifts or localized hot spots after rainfall or under high humidity. Additionally, fouling and partial contact occlusions raise the thermal time constant of substrate zones near the racks, producing slower thermal responses to irradiance fluctuations, as confirmed through time-resolved thermography. These findings highlight the critical influence of support structures on PV system durability and thermal behavior

Comparison of power loss factor of different priers: -

A comparative assessment of the power-loss factors associated with photovoltaic systems installed on different piers has done.

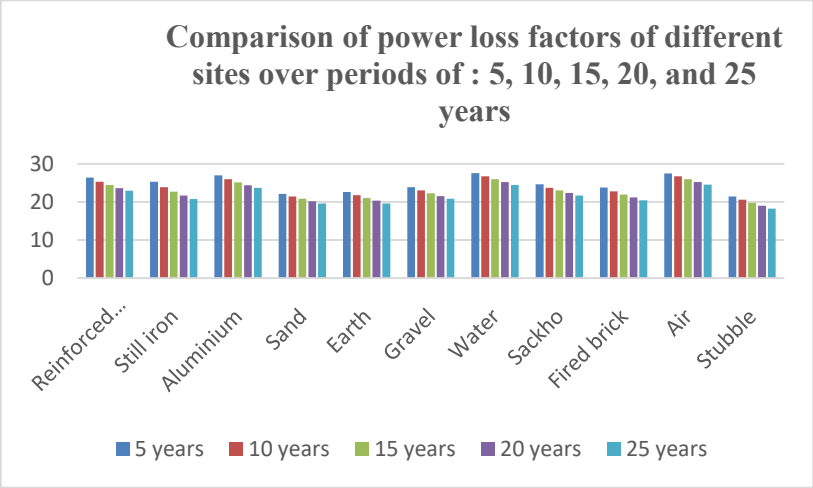

Figure 8. Comparison of relative power loss factors at different priers over periods of 5, 10, 15, 20, and 25 years.

Figure 8 presents the reduction rate of GPV power for different pier types over a 5- to 25-year period, evaluated in 5-year intervals. The results indicate that, for reinforced concrete, GPV performance remains largely unaffected by thermo-electric stresses during the first 5 to 10 years, likely due to the moderating influence of local climatic conditions. In contrast, air, water, and aluminum consistently emerge as the most favorable support materials, offering optimal conditions for maintaining and enhancing GPV performance.

Conclusion: -

This thesis assessed the long-term impact of different rack materials on the performance of a 300 Wp photovoltaic system through detailed simulation. The results show that installations supported by concrete, aluminum, air, and water provide the most favorable conditions for protecting the Back Surface Field (BSF) and sustaining optimal power production. In contrast, several other support structures significantly accelerate performance losses, highlighting their detrimental influence on PV efficiency. These findings demonstrate that the choice of mounting rack is not a trivial parameter but a critical determinant of system durability, thermal behavior, and electrical stability. Consequently, PV installations—particularly in residential settings—should no longer be mounted arbitrarily, as inappropriate support structures can contribute to voltage drops and long-term degradation of photovoltaic converters. This work underscores the need for informed selection of installation sites to ensure reliable and efficient PV operation over time.

Conflict of interest: -

The authors declare that they have no conflict of interest.

Acknowledgment: -

To theDean of the Faculty of Exact and Applied Sciences of Farcha-UNJ **Pr. NgarmaïnNadjitonon**, to the Manager of CNRD**Pr. Mahamoud Youssouf Khayal**, to the Managerof INSTA**Pr. Yaya Dagal Dari**, and the Manager of ONECS **Pr.BianzeubeTikri**and theManager of INSPEM**Dr. Alladj Hissein Issaka,** and Quality Control Manager of BDT **Mrs MBANDEGUE Koussidi Grace** for their contribution.

References: -

[1] D.C. Jordan, et al., Compendium of Photovoltaic Degradation Rates Prog. Photovoltaics Res. Appl., 24 (2016) P.978-989

[2] K. Aitola et al., Encapsulation of commercial and emerging solar cells with focus on perovskite solar cells. Solar Energy 237(2022) 264-283

[3] M. Al-Damook, et al., Evaluation of photovoltaic module efficiency: the case of Iraq Alex. Eng. J., (61) (2022) P.6151-6168

[4] T. Yamoussa et al., Comparative Study of Power Degradation in Five Photovoltaic Technologies Under Outdoor ConditionsConference. 13th International Conference on Smart Grid(2025)

[5] D. H. Daher et al., Experimental evaluation of long-term performance degradation of a photovoltaic power plant operating in a desert maritime climate Renew. Energy, 187 (2022) P.44-55
[6] Y. Y. Rady et al., Comparative Study of Power Degradation in Five Photovoltaic Technologies Under Outdoor Conditions: Case of Egypt. Energy 165(2018)
[7] [A. A. Mas'u et al., A Review on the Recent Progress Made on Solar Photovoltaics in Selected Countries of Sub-Saharan Africa. Renew. Sustain. Energy, 147 (2017) 358-367
[8] M. Taraba et al. Measurement of Thin-Film Solar Panel Properties under Adverse Weather Conditions. Transp Res Procedia 40 (2019) 535-540
[9] M. H. Adnan et al., Analysis and prediction of the performance and reliability of PV modules installed in harsh climates: case study Iraq, Renewable Energy 228(7)2024
[10] M. Taraba et al. Measurement of thin-film solar panel properties under adverse weather conditions Transp Res Procedia (2019)
[11] Un. Bouaichi, et al. In situ assessment of early degradation of photovoltaic modules of various technologies under harsh climatic conditions: the case of Morocco. Renew. Energy, 143 (Dec. 2019), pp. 1500-1518,
[12] E.J. Schneller et al. Manufacturing metrology for the reliability and durability of c-Si modules Renew Sustain Energy Rev (2016)
[13] M.B. Strobel et al. Uncertainty of photovoltaic performance parameters – location and material dependence Sol Energy Mater Sol Cells (2009)
[14] C. Baldus-Jeursen, A. Côté, T. Cerf, Y. Poissant Analysis of performance and lifecycle degradation of a 23-year-old photovoltaic module network in Quebec, Canada Renew. Energy, 174 (Aug. 2021), pp. 547-556
[15] D. C. Jordan, C. Deline, S.R. Kurtz, G.M. Kimball, M. Anderson Methodology and robust application of PV degradation. IEEE J. Photovoltaics, 8(2) 2018, p. 525-531
[16] Un. Bouaichi, and al. In situ evaluation of early degradation of photovoltaic modules of various technologies in harsh climatic conditions: the case of Morocco. Renewable Energy, 143 (Dec. 2019), p. 1500-1518
[17] D. H. Daher and al., Multi-faceted degradation analysis of a photovoltaic plant after 9.5 years of operation in hot desert climatic conditions. Prog. Photovoltaics Res. Appl., vol. 10 (2002)
[18] F. Martínez-Moreno, E. Lorenzo, J. Muñoz, and R. Moretón, "On the testing of large PV arrays," Prog. Photovolt: Res. Appl., vol. 20 (2012) P. 100–105
[19] G. H. Atmaram et al., Long-term performance and reliability of crystalline silicon photovoltaic modules. in Conference Record of the Twenty Fifth IEEE Photovoltaic Specialists Conference - 1996, Washington, DC, USA: IEEE, (1996), P. 1279–1282.
[20] M. J. Hahn, W. B. Berry, and L. Mrig, "Comparative short term/long term field test performance and stability of tandem and single junction a-Si modules," in IEEE Conference on Photovoltaic Specialists, Kissimmee, FL, USA: IEEE, (1990) P. 1057–1061.
[21] M. Ikisawa et al., Outdoor exposure tests of photovoltaic modules in Japan and overseas. Renewable Energy, vol. 14(1998) P. 95-100
[22] M. E. H. Jed et al., Analysis of the performance of the photovoltaic power plant of Sourdun (France). International Journal of Sustainable Engineering (2021) P. 1–13
[23] Accelerating the development of solar energy. EDF France (2021)
[24] Electricity Monthly Update - U.S. Energy Information Administration. EIA (2022)
[25] D. C. Jordan and S. R. Kurtz, "Photovoltaic Degradation Rates-an Analytical Review: Photovoltaic degradation rates," Progress in Photovoltaics: Research and Applications, vol. 21 (2013) P. 12–29
[26] S. S. Chandel, M. Nagaraju Naik, V. Sharma, and R. Chandel, "Degradation analysis of 28-years field exposed mono-c-Si photovoltaic modules of a direct coupled solar water pumping system in western Himalayan region of India," Renewable Energy, vol. 78 (2015) P. 193–202
[27] A. Chouder and S. Silvestre, "Automatic supervision and fault detection of PV systems based on power losses analysis," Energy Conversion and Management, vol. 51, no. 10 (2010) P. 1929 1937
[28] R. Dabou et al., "Monitoring and performance analysis of grid connected photovoltaic under different climatic conditions in south Algeria," Energy Conversion and Management, vol. 130 (2016), P. 200–206
[29] J. Leloux et al., "Monitoring 30, 000 PV systems in Europe: Performance, Faults, and State of the Art," in Proceedings of the 31st European PV Solar Energy Conference and Exhibition, Hamburg, Germany, 2015, pp. 14–18.
[30] IEC61724-1:2017. Photovoltaic System Performance Part 1: Monitoring; International Electrotechnical Commission. (2017)
[31] R. Srivastava, A. N. Tiwari, and V. K. Giri, "An overview on performance of PV plants commissioned at different places in the world," Energy for Sustainable Development, vol. 54 (2020), pp. 51–59